

NUMERICAL PROCESSES FOR IDENTIFICATION OF LANDSCAPE UNITS IN MONTANEOUS AREAS

Denis BLAMONT⁽¹⁾, Catherine MERING⁽²⁾ and Jean-François PARROT⁽²⁾

ABSTRACT

In montaneous areas, land cover, among other things depends on the versant exposure and the altitudinal distribution of vegetation. In those regions, spectral signatures of landscape units are also varying with the degree of illumination of the slopes while satellites are shooting. To take into account the last problem one can try to eliminate with appropriate treatments the shadow effects produced by topography introducing topographical data and a derivated illumination model. On the other hand, one can treat separately the topics according to the lighting. Their identification in areas presenting different degrees of illumination is to be done by a thresholding process according to radiometry and textural and structural parameters (variance and radiometric occurrence). We shall look then for correlations between spectral signatures belonging to a family of identical topics set in different conditions of lighting in the same altitudinal section.

RESUME

Dans les régions montagneuses, le couvert végétal dépend entre autres de l'exposition des versants et de l'étagement de la végétation. Dans ces régions, les signatures spectrales des unités de paysage varient également en fonction du degré d'éclairement des pentes lors des prises de vue satellitaires. Pour prendre en compte ce dernier problème, on peut tenter d'éliminer avec des traitements appropriés les effets d'ombre produits par la topographie en introduisant les données topographiques et les modèles d'ensoleillement qui en dérivent. En revanche, on peut traiter séparément les thèmes en fonction de l'éclairement. Leur identification dans des zones présentant différents degrés d'éclairement se fait par un processus de seuillage automatique tenant compte de la radiométrie et de paramètres de texture et de structure.

Fonds Documentaire IRD

Cote: Bx 25325 Ex: 1

(1) GRECO "Himalaya-Karakorum" CNRS. 1 place A. Briand F 92195 MEUDON Pal Cedex

(2) Télédétection ORSTOM 70-74 route d'Aulnay F 93140 BONDY



INTRODUCTION

Land use generally depends on the nature of soils, climate, hydrographic nets and human interventions. In montaneous areas it depends moreover on the altitudinal distribution of vegetation, on exposure of versants and the degree of slopes.

In these regions, spectral datas from MSS-bands are affected by the hour of shooting and by the illumination of slopes depending on the topography. Over Himalaya of the Center of Nepal (cf. fig. 1), the LANDSAT satellite always flies about 9.20 a.m. At this moment, according to seasons, azimuth and sun elevation are varying respectively between 140° and 90° and between 30° and 60° . These variations involve modifications of the angle of incidence and of the direction of the rays : some versants are whether illuminated or in the shadow. However, steep slopes on westwards versants will always be in the shade (the light being more or less grazing on soft slopes) and eastwards versants will always be illuminated.

We first have isolated the radiometric themes studying them in their environment using the MSS data. These themes are the result of an automatic thresholding of one of the MSS-band combined with variables derived from the radiometry measures, such as texture index. The unsupervised classification depends on the spatial arrangement of the radiometric values of the pixels, depending itself on the arrangement of the various landscape units on the ground.

The process itself is based on the calculation of the following variables :

- . local radiometric occurrence in a (mxm) matrix,
- . the mean radiometric occurrence within a window;
- . the thresholding of this last function,
- . the variation coefficient in a (mxm) matrix.

In the second part, we took into account the support of the landscape units; we replaced them in various altitudinal portions and in various classes of illumination, using topographic data.

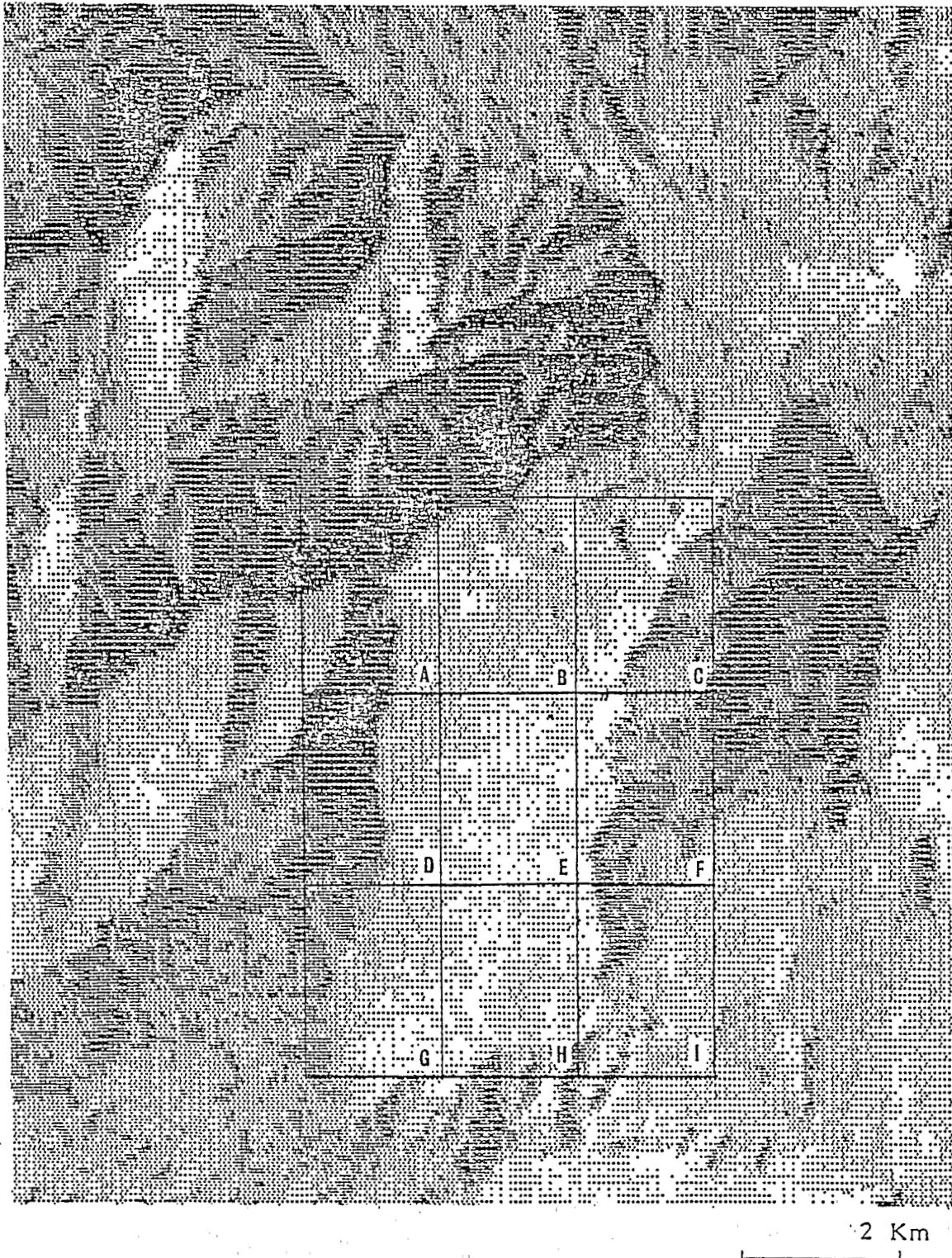


Figure 1. Localization of the studied area on MSS7.

The interpretation of the themes in term of landscape units is done afterwards, according to our knowledge of training areas on the ground.

CONCEPTS AND TOOLS

Thresholding

Difficulties encountered during treatments of MSS data on vegetal cover of himalayan regions start with the initialization of standart methods of classification. As we said above in this paper, according to lighting and slope, a same theme on the ground will surely not have the same radiometric answer in any of the four bands⁽¹⁾. Therefore we studied radiometry in connection with textural elements.

At this very point, the problem of the thresholding technique appeared to us. As a matter of fact, very few classification methods on satellitary images can avoid this preliminary stage. Usual methods of thresholding images such as inter-active thresholding depending only on the visualization of a band on a video screen or statistical thresholding depending of the statistical distribution of a band within a window, were not satisfactory in our case.

Local radiometric occurrence

It appeared to us necessary to introduce, during the process of thresholding MSS-bands, variables indicatory of the spatial arrangement of a given radiometrical value. That is why we have defined the local radiometric occurrence on a square matrix (mxm) centered on a pixel i as the occurrence $c(i)$ of the more frequent radiometric value within the matrix (mxm) centered on pixel i , for any MSS-band.

(1) J.V. DAVE and R. BERNSTEIN, 1982.

Mean radiometric occurrence within a window

This function is defined for each radiometric value n , in one of the four MSS-bands, within a squared window $N \times N$ from the Landsat scene. It needs the calculation of local radiometric occurrence $c(i)$.

$$\text{HISTC}(n,N) = \frac{\sum_{i=1}^{N^2} c(i) \delta_i^n}{\sum_{i=1}^{N^2} \delta_i^n}$$

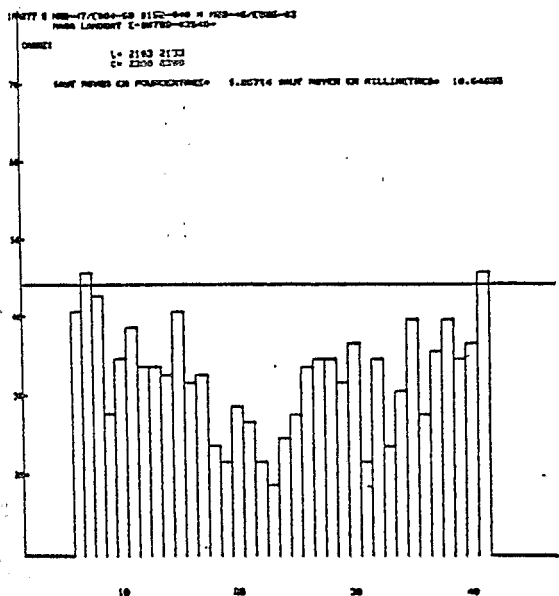
$c(i)$ is the local radiometric occurrence of the pixel occupying the i^{th} position in the scanning of the window according to columns and then rows.

We will threshold this last function in order to initialize the clustering of the themes (cf. fig. 2).

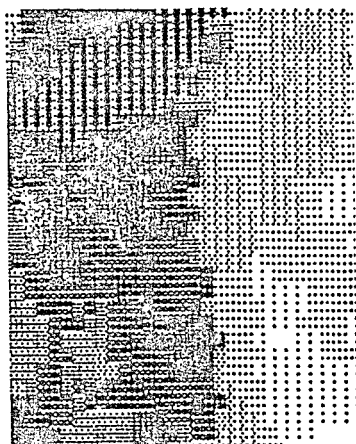
The maxima correspond to radiometric values occurring in the window and having the highest occurrence in a given geometrical neighbourhood within this window. The minima correspond whether to transition areas such as valley bottoms or crest lines, whether to heterogeneous themes on the ground, or to quickly changing illumination on one theme, according to topography.

Thresholding of function HISTC(N,n)

This function is not correlated to a statistical distribution. Therefore we shall not consider modes or minima. In another hand we can associate the absolute difference between two consecutive values of this function. The larger is the difference, the more various are the spatial

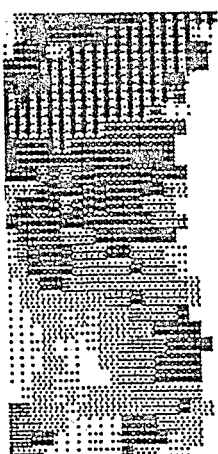


2

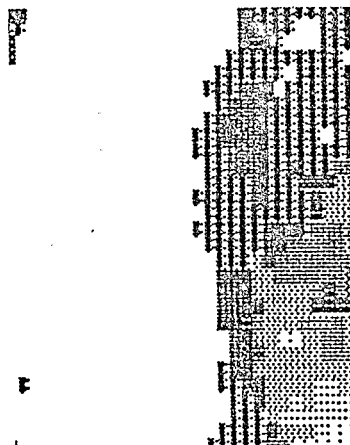


4

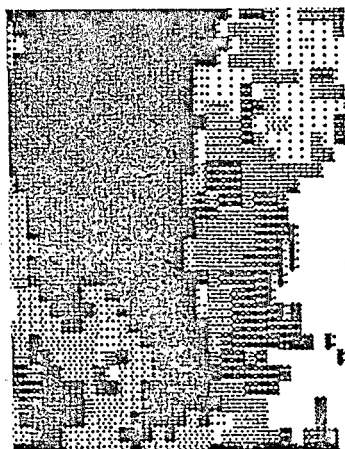
1 Km



3A



3B



5

Fig. 2. HISTC

Fig. 3. Thresholding MSS6 by the criterium of the absolute difference (5%).

A. Shady slope

B. lighted slope

Fig. 4. Thresholding MSS6 by the criterium of the mean difference.

Fig. 5. Thresholding green vegetation index.

arrangements of the corresponding radiometric values in the window. The criterium used in the thresholding is relative to the window : it is the mean difference between consecutive values occuring within the whole window.

Variation coefficient in a matrix mxm

The calculation of $c(i)$ and HISTC(n,N) does not take into account the absolute difference between radiometric values of a group of pixels set in the same geometric neighbourhood. Elementary simulations⁽¹⁾ show that for a given spatial arrangement of pixels and for a given n affecting this pixels, the function HISTC(n,N) has various items according to the degree of heterogeneity of the immediate neighbourhood.

As a matter of fact, the calculation of HISTC(n,N) could be applied to any qualitative variable such as the result of a classification but it does not use the property of measure of the radiometric variable. That is why we had to calculate the local standart deviation on a (mxm) matrix, $\sigma(i)$, for every pixel i of the window. In our case this parameter will systematically be higher inside a matrix containing illuminated pixels than inside one containing pixels in shadow. Therefore we also calculated the coefficient of variation covi(i) inside a matrix (mxm) balanced by a constant K chosen by the operator.

$$covi(i) = \frac{\sigma(i)}{\mu(i) + K}$$

where $\mu(i)$ is the mean of the m^2 values in the matrix (mxm) centered on the pixel i and $\sigma(i)$ the corresponding standart deviation.

This parameter becomes a new quantitative variable used in the classification of pixels at the same time with MSS band-variables.

(1) We have calculated that, for a given value n affecting a set of pixels drawing a given shape, the function HISTC(n,N) can be 1,3 higher when the immediate neighbourhood of that shape is heterogeneous than when the neighbourhood is an homogeneous set (ie. with the same radiometric value).

METHODOLOGY. RESULTS

Preliminary remarks

The mean radiometric occurrence has been calculated, for each value of one MSS-band in a set of training areas (cf. fig. 1) the size of which is 30 by 30 pixels. The matrix coming into the calculation of local occurrence and local coefficient of variation is a 3x3 matrix.

Three types of thresholding have been employed. In all cases, one tests the acceptable limits of variability of HISTC(n,N) between consecutive values in order to aggregate these values associated then to the reflectance variability of a same theme.

The two first thresholdings use an absolute criterium : one aggregates two consecutive values if the difference between the corresponding values of HISTC is greater than five per cent of the maximum difference, and then ten per cent of this maximum.

This technique is available in presence of series of continuums of the function separated by sensible differences as it happens for training areas separated in two parts by a crest line or a valley bottom, and containing a great amount of various themes.

But in other cases HISTC has a small variability in comparison with the maximum and we finally applied the criterium of the mean difference relative to the window inside which is calculated HISTC.

The criterium of ten per cent is not able to isolate the versants in the shadow or some illuminated themes. On the other hand the criterium of five per cent leads to a scattering of the illuminated themes (cf. fig. 3A and 3B). Moreover, in some areas, HISTC has such a small variability that these criteriums can hardly isolate more than one theme. A part from this extreme case, the mean differences of HISTC within various windows are generally included between the two criteriums seen above.

We applied the mean difference criterium on the MSS-6 data (cf. fig. 4) and then on the green vegetation index (cf. fig. 5) in the same window.

Classification process

Having thresholded HISTC on one of the MSS-bands, we introduced the coefficient of variation $covi$ in an hypercubic classification⁽¹⁾ process combined with the result of the HISTC thresholding. $Covi$ has been thresholded within three levels. By this way, we define on every training window, areas of small coefficient of variation (they correspond to zones in which the standart deviation is small or equal to zero), areas with a high coefficient (generally corresponding to lineaments underlining more frequently the crossing from shadow to light) and areas with a mean coefficient.

The value of constant K depends on the calibration scale of each MSS-band. One uses K to balance the difference of the grey level scales between shadow and light in the calculation of the coefficient of variation.

The combination of the thresholding of HISTC and of the three-levels-thresholding of the coefficient of variation involves that one grey level (ie. one class) defined on a MSS-band can be subdivided within three sub-classes. Comparative statistics on these sub-classes give indications about the spatial arrangement of pixels affected by the same grey level.

Therefore, it is not only a cartographic document that can be supplied by this process, but also criteriums allowing thematicians to analyse the classified themes.

Results

In order to illustrate the results, we have chosen samples chiefly showing the oak forests between 2000 and 3500 meters. Moreover, we only analysed the west-north-west and east-south-east versants, that is to say the ones that are perpendicular to the solar azimuth at the shooting time.

In this sample, the treatment has been applied on MSS5 and MSS6 bands inside two contiguous windows (window D and window B).

Inside window D corresponding to an essentially shady area (cf. fig. 6), the algorithm supply 21 sub-classes on the shady versant and 30 sub-classes on the illuminated one.

(1) ORSTOM (1978)

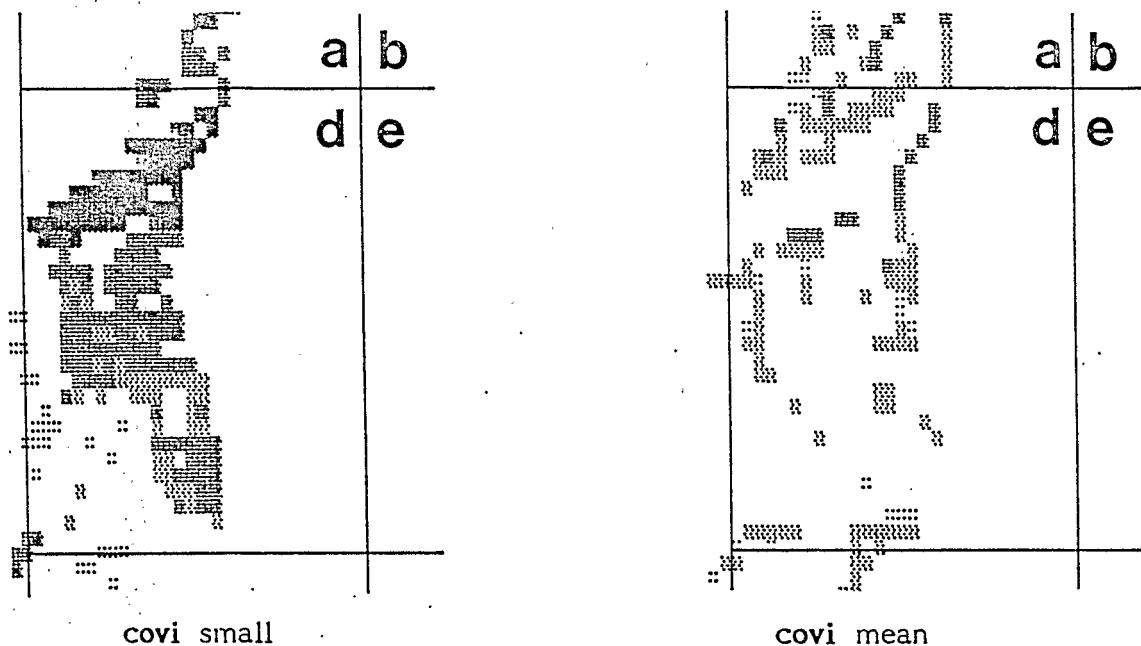


Figure 6. Map obtained by hypercubic treatment MSS6/covi ($K = 50$) based on the thresholding on training window D.

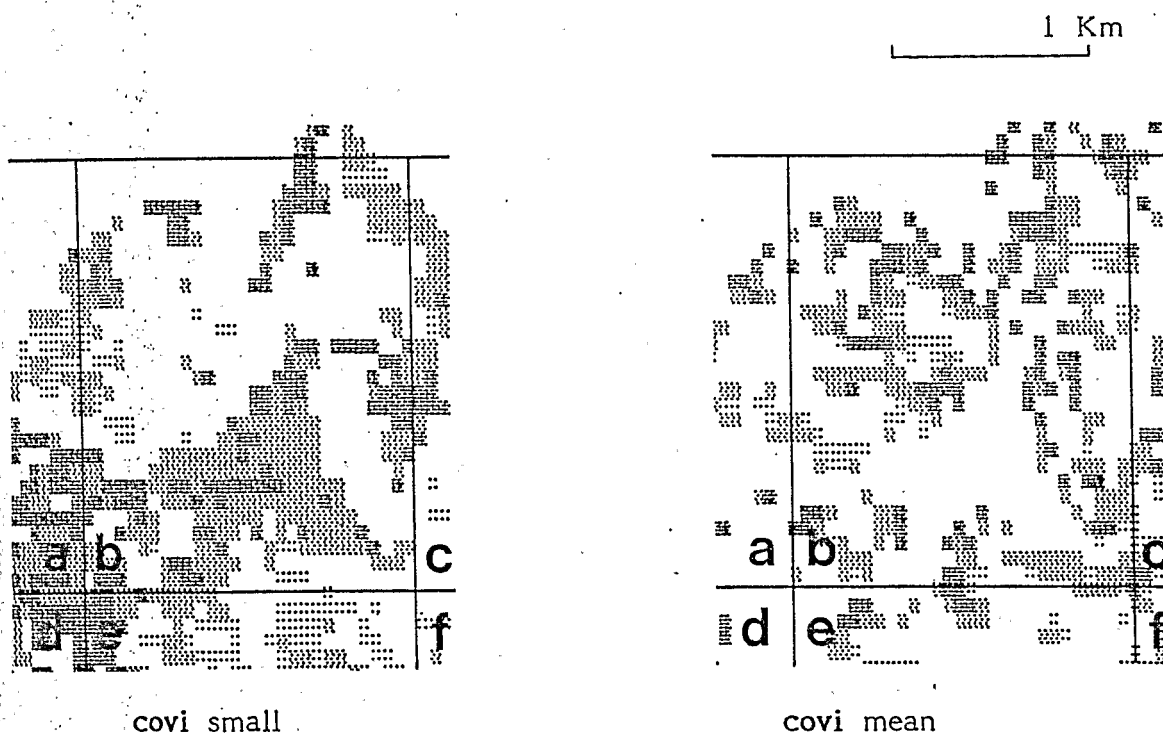


Figure 7. Map obtained by hypercubic treatment MSS6/covi ($K = 50$) based on the thresholding on training window B.

The following table gives the characteristics of each sub-class when the constant K is equal to 50 :

TABLE I

Sub-class	Radiometry	Value of HISTC	Coeff. var.	% inside window
1	6 to 8	44	small	6.22
2	6 to 8	44	mean	1.55
3	6 to 8	44	high	0.33
4	9	27	small	1.11
5	9	27	mean	1.00
6	9	27	high	0.33
7	10 to 14	36	small	10.66
8	10 to 14	36	mean	8.11
9	10 to 14	36	high	1.22
10	15	41	small	4.22
11	15	41	mean	1.22
12	15	41	high	0.33
13	16/17	33	small	2.33
14	16/17	33	mean	4.11
15	16/17	33	high	1.00
16	18/19	24	small	0.66
17	18/19	24	mean	2.66
18	18/19	24	high	0.33
19	20/21	37	small	1.33
20	20/21	37	mean	2.00
21	20/21	37	high	0.88

nota : the three-levels-thresholding of the coefficient of variation has the following values : 0 to 2, 3 to 6, above 6.

In window B (cf. Table II), where landscape units are again forests mainly on an illuminated zone (cf. fig. 7), 38 non empty sub-classes are supplied (among which 24 sub-classes are included in illuminated areas)

The same treatment has been processed on MSS5-band (cf. fig. 8) where we can notice that the classes are bigger and not so numerous than with MSS6. MSS6 supply more informations inside classes than MSS5.

Furthermore, the green vegetation index has been processed by the same way.

TABLE II

Sub-class	Radiometry	Value of HISTC	Coeff. var.	% inside window
			small	0
			mean	0.22
			high	0.11
11	20	11		
12	20	11		
			small	0
			mean	2.66
			high	0.66
13	21 to 23	28		
14	21 to 23	28		
			small	0.11
			mean	1.55
			high	0.33
15	25	30		
16	25	30		
17	25	30		
			small	0.11
			mean	0.88
			high	0.22
18	26	17		
19	26	17		
20	26	17		
			small	3.66
			mean	4.88
			high	0.44
21	27.28	26		
22	27.28	26		
23	27.28	28		
			small	10.11
			mean	6.55
			high	0.55
24	29.30	35		
25	29.30	35		
26	29/30	35		
			small	23.22
			mean	19.11
			high	0.33
27	31 to 36	30		
28	31 to 36	30		
29	31 to 36	30		
			small	5.44
			mean	6.00
			high	0
30	37 to 39	32		
31	37 to 39	32		
			small	1.44
			mean	2.11
			high	0
32	40/41	28		
33	40/41	28		
			small	0
			mean	1.00
			high	0
34	42	36		
	42	36		
	42	36		
			small	0.88
			mean	1.00
			high	0
35	43	30		
36	43	30		
	43	30		
			small	0.11
			mean	0.22
			high	0
37	46	21		
38	46	21		
	46	21		

Thematic interpretation

Covi being applied pixelwise, whereas the thresholding of HISTC is done for the whole window, the classification of the pixels in one of the three sub-classes allows to identify them as precise landscape units. The pixels classified in one small *covi* sub-class are representative of one landscape unit (ie. dense oak forest on lighted slopes).

The pixels which are classified in the mean *covi* sub-classes are, when isolated, transition between two landscape units (ie. dense forest and degraded forest), and, when spatially grouped, heterogeneous units : some of the classes identified by the thresholding of HISTC do even have the majority (if not the totality) of their pixels comprised in the mean *covi* sub-class (cf. sub-class n° 14, 17 and 20 of Table I; and sub-class 11, 13, 16, 19, 22, 31, 33, 34, 36 and 38 of Table II). They are representative of heterogeneous (ie. degraded forest) and transition units (ie. degraded forest in the valley bottoms) between two equally or even more heterogeneous units.

The pixels classified in high *covi* sub-classes are representative of limits between lighted and shady slopes when in lines; and, when grouped, representative of vegetation units on versants where light is grazing. As the quick variation of radiometry due to variations of lighting conditions prevents their correct mapping during the general process, they will have to be treated separately : the classes representing very homogeneous landscape units do not have in this case the majority of their pixels in the small *covi* sub-classes.

This method allows then to map satisfactorily oak forests (according to their density and stages), their limits with other landscape units (cultivated areas, pastures...), other degraded forests and some cropped areas, regardless of the lighting, on the training window.

The classification thus obtained from the MSS6 data has to be made up with a similar classification on other MSS-bands, even on values like green vegetation index, to allow its extension to the whole area.

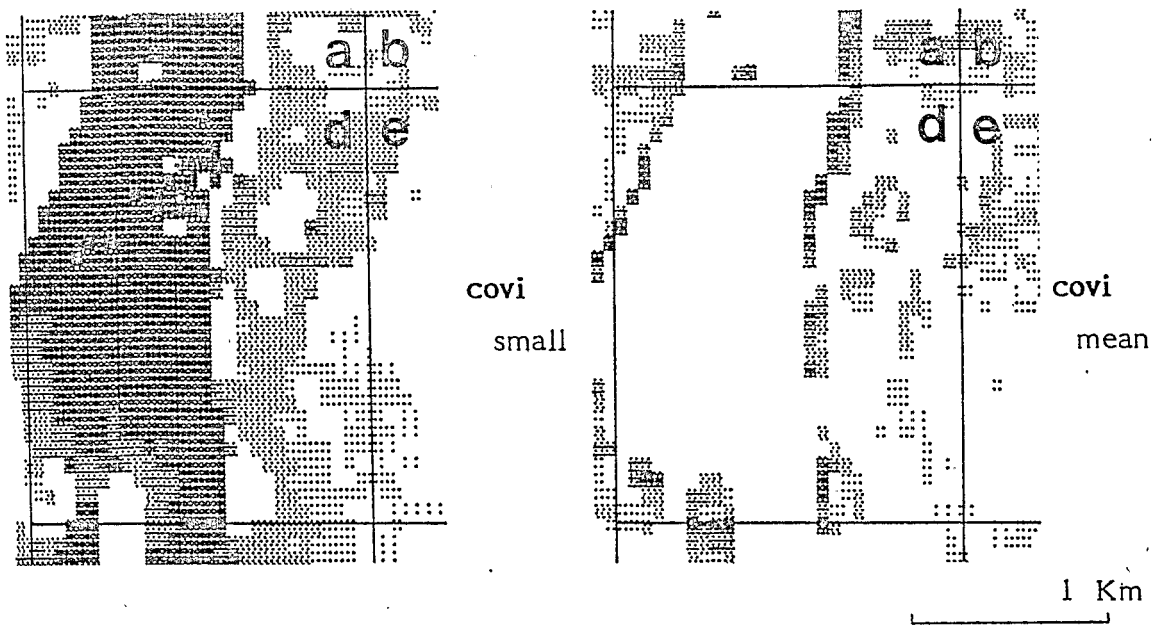


Figure 8. Map obtained by hypercubic treatment MSS5/covi ($K = 50$) based on the thresholding on training window D.

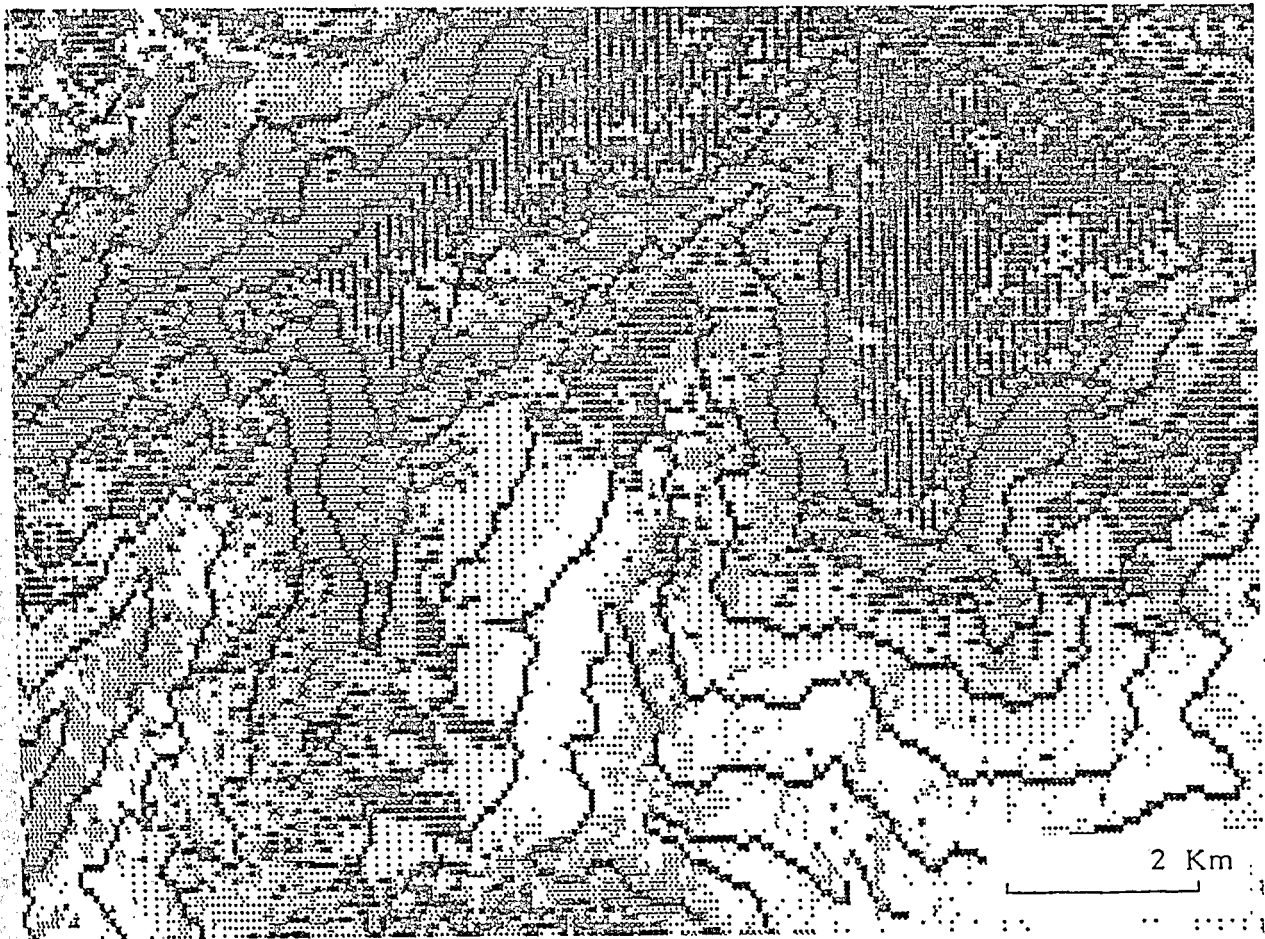


Figure 9. Supervised hypercubic treatment green vegetation index/altitudes.

ALTITUDE AND TOPOGRAPHY

Although our purpose in this paper is limited to the study of a certain type of landscape units in determined altitudinal portions, we will briefly talk about the use of topographic data and illumination classes in a simple way.

Altitudinal portions

The figure 9 shows a supervised classification on green vegetation index combined with a subset of topographic data. It is then possible to map different landscape units (high leveled pastures or low altitude wheat fields for exemple) which were classified as only one theme before.

Of course this process can be applied to altitudinal portions whether systematically or by selecting portions corresponding to known facts on the ground (ie. known change of vegetation type at a certain altitude, and so on).

Illumination classes

An unsupervised treatment can also be processed combining the results of the classification described above and classes of illumination. These classes are supplied applying the following model to topographic data⁽¹⁾ :

$$\text{class} = \text{CS}(Z) + \text{CR}(i) + \text{CSOL}(i) + \text{OMBRE}(i)$$

where :

$\text{CS}(Z)$ = absorption coefficient (function of the altitude of the point)

$\text{CR}(i)$ = absorption coefficient (function of the sun elevation)

$\text{CSOL}(i)$ = projection of the sunbeam on the normal to the ground

$\text{OMBRE}(i) = . 0$ when the point is in the shadow

$. 1$ when the point is under the sun.

i depends on the hour of the shooting.

(1) This model has been calculated by IGN (French National Geographic Institute).

Another simple application is to map the themes in a stochastic process for a same illumination class.

CONCLUSION

The utilized processes on LANDSAT data made possible a satisfactory automatic mapping of vegetation units in an himalayan mountaneous area regardless of the lighting conditions within working windows because they are based on the consideration of not only the radiometry but also the index of local repartition of radiometric values and the index of mean spatial repartition of radiometric values in the working window.

The introduction of exogeneous data such as altitude allows to remove the ambiguities remaining after the processing of the treatment to a larger area.

REFERENCES

- BLAMONT D. (1982) .- Cartographie de la végétation et de l'occupation des sols au Népal Central à partir d'images LANDSAT acquises en mars 1977. IV Coll. internat. GDTA, Toulouse (1981) : 222-229.
- BLAMONT D., MERING C. et PARROT J.-F. (1983) .- Essai de classification des unités de paysage en région montagneuse (Centre du Népal). Coll. "Géographie, Aménagement et Télédétection spatiale, Chantilly (1983).
- DOBREMEZ J.-F., MAIRE A. et ION B. (1982) .- Carte écologique du Népal (5) Région Aukhu-Khola-Trisouli, 1/50 000. Doc. Cartogr. écologique Grenoble, 15 : 1-20.

- DAVE J.V. and BERNSTEIN R. (1982) .- Effect of terrain orientation and solar position on satellite level luminence observations. Remote Sensing of Environment, 12, n° 4 : 331-347.
- FLOUZAT G. (1982) .- Modélisation de la compréhension visuelle des images en Télédétection : essai de simulation numérique de la photo-interprétation analytique. Symp. internat. Commission VII SIPT, Toulouse (1982), 24 : 7-24.
- HOLBEIN B.N. and JUSTICE C.O. (1980) .- The topographic effect on spectral reponse from Nadir-pointing sensors. Photogram. Eng. and Remote Sensing, 46, n° 6 :1191-1199.
- JEANSOULIN R. (1982) .- Les images multisources en Télédétection. Thèse Doct. es Sci., 127p. multigr.
- JUSTICE C.O., WHARTON S.W. and HOLBEIN B.N. (1981) .- Application of digital terrain data to quantify and reduce the topographic effect on Landsat data. Internat. J. of Remote Sensing, 2, n° 3 : 213-230.
- MAUER E. and SCHARF R. (1982) .- Picture classification and segmentation by feature combination in multispectral data. Symp. Internat. Commission VII SIPT, Toulouse (1982) 24 : 35-43.
- ORSTOM (1978) .- Analyse multivariable. Procédure "Loterie". Application à l'analyse multispectrale en Télédétection. Init. Doc. Tech. ORSTOM, 39, Télédétection, n° 2, 78 p.

NUMERICAL PROCESSES FOR IDENTIFICATION OF
LANDSCAPE UNITS IN MONTANEOUS AREAS

XXXXX

Denis BLAMONT⁽¹⁾, Catherine MERING⁽²⁾ and Jean-François PARROT⁽²⁾

x x x

Paper presented at
the XV International Congress of ISPRS
(Rio de Janeiro, 17-29 June 1984)

(1) GRECO "Himalaya-Karakorum" CNRS 1 place A. Briand F 92195 MEUDON Pal Cedex
(2) Télédétection ORSTOM 70-74 route d'Aulnay F 93140 BONDY



International Society for Photogrammetry and Remote Sensing

XVth Congress

Société Internationale de Photogrammétrie et de Télédétection

XV^e Congrès

Internationale Gesellschaft für Photogrammetrie und Fernerkundung

XV. Kongress

INTERNATIONAL ARCHIVES OF PHOTOGRAMMETRY AND
REMOTE SENSING

ARCHIVES INTERNATIONALES DE PHOTOGRAMMETRIE
ET DE TELEDETECTION

INTERNATIONALES ARCHIV DER PHOTOGRAMMETRIE
UND FERNERKUNDUNG

Volume

Volume

Band

XXV

Part

Tome

Teil

A7

Commission

Commission

Kommission

VII

Fonds Documentaire IRD

Cote : Bx 25325 Ex : 1

Published by the Committee of the XVth International Congress of Photogrammetry and
Remote Sensing

Publié par le Comité du XV^e Congrès International de Photogrammétrie et de Télédétection

Herausgegeben von dem Komitee für den XV. Internationalen Kongress der Photogrammetrie
und Fernerkundung

COMMISSION/KOMMISSION VII

INTERPRETATION OF PHOTOGRAPHIC AND REMOTE SENSING DATA

INTERPRETATION DE DONNEES PHOTOGRAPHIQUES ET DE TELEDETECTION

INTERPRETATION DER INFORMATIONEN AUS PHOTOGRAPHIEN UND FERNERKUNDUNG

<u>AUTHOR/AUTEUR/AUTOR</u>	<u>CONTENTS/MATIERES/INHALT</u>	<u>PAGE/SEITE</u>
ALLAN, J.A.	MONITORING CHANGES IN LAND COVER IN SEMI-ARID REGIONS BY REMOTE SENSING TECHNIQUES	1
AMADESI, E. CASALICCHIO, G. VIANELLO, G.	METHODOLOGY OF ENVIRONMENTAL RESEARCH FOR NEW SETTLEMENTS IN THE EASTERN SULAWESI (INDONESIA)	7
AOKI, H. SARAIVA, I.R. MOTA, I.S. FAVRIN, L.J.B.	VOLUME ESTIMATES OF ARAUCARIA ANGUSTIFOLIA (BERT.) O.KTZE. USING AERIAL PHOTOGRAPHS	16
AOKI, H. SARAIVA, I.R. SANTOS, J.R. HERNANDEZ F., P.	WILD AREAS MONITORING USING LANDSAT DATA	27
ASHWORTH, M. CHIDLEY, T.R.E. COLLINS, W.G.	VISUAL ANALYSIS OF DIGITAL IMAGES FOR STUDIES IN WATER RESOURCES	36
AXELSSON, S.R.J.	IMPROVED MODELING OF THE MICROWAVE RADIOMETRIC RESPONSE OF BARE GROUND	46
AXELSSON, S.R.J.	THERMAL-IR EMISSIVITY OF SOILS AND ITS DEPENDENCE ON POROSITY, SURFACE ROUGHNESS AND SOIL-MOISTURE	56
BAOXI, Z.	APPLICATION OF REMOTE SENSING IMAGERY INTERPRETATION IN RAILWAY SURVEYING	65

BARSCHE, H.
MAREK, K.H.
SÖLLNER, R.
WEICHELT, H.

INVESTIGATION OF SPECTRAL
CHARACTERISTICS OF NATURAL OBJECTS
IN TESTSITES OF THE GDR

75

BINAGHI, C.M.V.
VIOLA, A.B.
BROONER, W.G.

LANDSAT MONITORING OF TEMPORAL
HIDROLOGICAL VARIATIONS AND ACTUAL
LAND USE ON THE LAGUNA YEMA AREA
(FORMOSA PROVINCE, ARGENTINA)

85

→ (BLAMONT, D.
MERING, C.
PARROT, J.F.)

NUMERICAL PROCESSES FOR
IDENTIFICATION OF LANDSCAPE UNITS
IN MONTANEOUS AREAS

94

CIESLA, W.M.

PANORAMIC AERIAL PHOTOGRAPHY FOR
MAPPING HARDWOOD DEFOLIATION BY
GYPSY MOTH IN THE NORTHEASTERN
UNITED STATES

111

COHEN, W.B.
ASHLEY, M.D.

CONIFEROUS REGENERATION SURVEYS
USING COLOR INFRARED AERIAL
PHOTOGRAPHY

124

COWAN, A.M.
ULBRICHT, K.A.

SATELLITE IMAGERY ANALYSIS OF ICE
EDGE EDDY DYNAMICS

134

CSAPLOVICS, E.

A PRACTICAL APPLICATION OF COLOUR
INFRARED (IR) IMAGE INTERPRETATION
-THE CLASSIFICATION OF THE REED OF
LAKE NEUSIEDL (AUSTRIA)

143

DERENYI, E.E.
STUART, A.J.

GEOMETRIC ASPECTS OF SPACEBORNE
STEREO IMAGING RADAR

153

EHLERS, M.
DENNERT-MÖLLER, E.
KOLOUCH, D.
LOHMAN, P.

NONRECURSIVE FILTER TECHNIQUES IN
DIGITAL PROCESSING OF REMOTE
SENSING IMAGERY

163

ELMAN, R.I.
KUZENKOV, L.A.
BODANSKIY, E.D.

MAN/MACHINE INTERACTION DURING
FOREST IMAGE PROCESSING

176

FAVRIN, E.J.B.

QUANTITATIVE ANALYSIS OF THE VEGETATION
COVER ALTERATION IN THE CAMPOS DO JOR -
DÃO-COUNTY

181

FORESTI, C. OLIVEIRA, M.L.N. NIERO, M. PARREIRA, E.M.M.F.	THE USE OF AN IMAGE REGISTRATION TECHNIQUE IN THE URBAN GROWTH MONITORING	192
FORMAGGIO, A.R. SANTOS, J.R. DIAS, L.A.V.	PRINCIPAL COMPONENTS TECHNIQUE ANALYSIS FOR VEGETATION AND LAND USE DISCRIMINATION	197
FORSTER, B.C.	COMBINING ANCILLARY AND SPECTRAL DATA FOR URBAN APPLICATIONS	207
GODOI, S.S. STEVENSON, M.R.	SEASONAL OSCILLATIONS OF THE SUBTROPICAL CONVERGENCE BETWEEN THE BRAZIL AND MALVINAS CURRENTS, USING OCEANOGRAPHIC AND SMS-2 SATELLITE DATA	217
GRIFFITHS, G.H. COLLINS, W.G.	MAPPING THE GREENNESS OF SEMI-ARID RANGELAND VEGETATION IN NORTHERN KENYA FROM LANDSAT DIGITAL DATA	227
HÄME, T.	INTERPRETATION OF DECIDUOUS TREES AND SHRUBS IN CONIFER SEEDLING STANDS FROM LANDSAT IMAGERY	237
HILDEBRANDT, G.	ASPECTS OF COUNTRY WIDE INVENTORY AND MONITORING OF ACTUAL FOREST DAMAGES IN GERMANY	246
KIENKO, J.P.	REMOTE SENSING AS A TOOL FOR NATURE INVENTORY	268
KÖLBL, O. STUBY, J.J.	ANALYSE DES TERRAINS INSTABLES A L'AIDE DE PHOTOGRAPHIES AERIENNES DIACHRONIQUES	272
KONNECNY, G. DENNERT-MÖLLER, E. EHLERS, M. KÓLOUCH, D. LOHMANN, P.	METHODS AND POSSIBILITIES OF REMOTE SENSING IN COASTAL AREAS	281
LEE, D.C.L. HERNANDEZ Fº, P. SHIMABUKURO, Y.E. ASSIS, O.R. MEDEIROS, J.S.	FOREST INVENTORY USING MULTISTAGE SAMPLING WITH PROBABILITY PROPORTIONAL TO SIZE	285

LIU, J.	TWO NEWLY-DISCOVERED TECTONIC PATTERNS IN TAIWAN REGION-THE CIRCULAR PATTERN AND THE NW-SE SHEAR ZONE - AS INTERPRETED FROM SMALL-SCALE REMOTE SENSING IMAGES	293
LOHMANN, P.	THERMAL MAPPING OF COASTAL WATERS	303
LU, J. CHENG, W.	THE ESTUARINE PROCESSES OF THE TATU RIVER-TAICHUNG, TAIWAN - BY REMOTELY SENSED DATA ANALYSIS	315
MOHL, H. SCHWEBEL, R.	THE ZEISS STEREOCORD FOR MANIFOLD MEASURING INTERPRETATION APPLICATIONS	325
MOREIRA, M.A. CHEN, S.C. BATISTA, G.T.	SAMPLING SYSTEM FOR WHEAT (TRITICUM AESTIVUM L) AREA ESTIMATION USING DIGITAL LANDSAT MSS DATA AND AERIAL PHOTOGRAPHS	336
MURALIKRISHNA, I.V.	STUDY OF LARGE SCALE TIDAL VORTICES THROUGH REMOTE SENSING	347
MURTHA, P.A.	REPORT OF THE WORKING GROUP : ON VEGETATION DAMAGE	358
MURTHA, P.A.	STRAIN SYMPTOM PATTERNS OF SPRUCE BEETLE - ATTACKED SPRUCE	364
NEGUT, N. BALTEANU, D. MIHAIU, G. CAPLESCU, L. BALANESCU, P. SAVULESCU, C.	PHOTOGRAMMETRIC METHODS IN GEOMORPHOLOGICAL PROCESS STUDIES. A CASE STUDY FROM ROMANIAN SUBCARPATHIANS	379
NIEUWENHUIS, E. SHRESTHA, D.	AN EXERCISE IN SOIL SURVEY AND LAND EVALUATION USING DIGITAL PROCESSING AND IMAGE INTERPRETATION	387
NOVAKOVSKI, B.A.	PHOTOGRAMMETRIC PROBLEMS OF JOINT APPLICATION OF AERIAL-SPACE IMAGERY AND CARTOGRAPHY METHODS FOR THE STUDY OF THE NATURAL RESOURCES	397

OHNUKI, I. AWAYA, Y. SAWADA, H.	LANDSAT DATA FOR PRACTICAL DEFORESTATION DETECTION - A TEST CASE	404
OLIVEIRA, M.L.N. BARROS, M.S.S.	THE USE OF PHOTOINTERPRETATION FOR SOCIO-ECONOMIC CHARACTERIZATION OF URBAN POPULATION	412
OPRESCU, N. MANDESCU, E.	DETERMINATIONS SOUS-SATELLITAIRES RADIOMETRIQUES ET D'INDICATEURS DES OBJETS EN VUE DE L'APPLICATION DE CORRECTIONS AUX ENREGISTREMENTS DE TELEDETECTION	418
PATMIOS, E.	PHOTOINTERPRETATION OF LANDSAT IMAGES	424
PESHA, V.V. KALE, V.S	GEOLOGICAL INTERPRETATION OF BHASKARA-II (ISPRO) IMAGERIES: A COMPARATIVE STUDY OF THE RESULT USING LANDSAT IMAGERIES AND AERIAL PHOTOGRAPHS	428
QUIEL, F.	TRENDS AND DEVELOPMENTS IN THE CLASSIFICATION OF MULTISPECTRAL DATA	440
RIVEREAU, J.C.	SPOT IMAGERY, FUTURE PRODUCTS AND POTENTIAL APPLICATIONS	452
SÖLLNER, R. MAREK, K.H. SIEBERT, R. SCHMIDT, K.	ON THE EXTRACTION OF TEXTURAL AND STRUCTURAL FEATURES IN REMOTE SENSING DATA	471
SUKHIKH, V.I.	AIR SPACE METHODS APPLICATION FOR FOREST STUDY AND CARTOGRAPHY	481
SZORENYI, J.A.	GEOMETRIC CORRECTION OF LANDSAT MSS IMAGERY	483

TAHERKIA, H.
MORTON, J.
COLLINS, G.

SLOPE STABILITY IN MOUNTAINOUS
ROADS IN IRAN. A CASE FOR REMOTE
SENSING?

495

THORÉN, R.

APPLICATIONS OF REMOTE SENSING
TECHNIQUES TO OCEANOGRAPHY AND SEA
ICE

504

VERMA, V.K.
PRASAD, C.
RAWAT, G.S.

STUDY OF ALLUVIAL AND TALUS FANS
IN HIMALAYA BY REMOTE SENSING
TECHNIQUES

514

WU, S.S.C.

MAPPING FROM SHUTTLE IMAGING RADAR,
SIR-B, EXPERIMENT

521